Discrete and Continuous Dynamical Systems - Series S

doi:10.3934/dcdss.2025076

BIFURCATION ANALYSIS ON IMMUNOTHERAPY OF A TUMOR MODEL WITHOUT TREATMENT

Ruchita Amin[✉] and Pei Yu[✉*]

Department of Mathematics, Western University, London, Ontario, N6A 5B7, Canada

Abstract. Immunotherapy is one of the most methodologies developed recently for reducing and alleviating the dangerous growth of tumors. In this paper, we explore bifurcation analysis on a tumor mathematical model including $CD4^+$ T cells and cytokines. The case without treatment is studied in order to estimate the limitation of a successful therapy. Particular attention is focused on the existence of equilibrium solutions and their stability. Bifurcation diagrams are used to consider the inter-individual variability for a non-treatment situation, showing the existence of oscillating behaviors due to Hopf bifurcation. It is shown that patients with very low tumor antigenicity experience tumors expanding to its maximum size, regardless of whether the tumor destruction rate and cytokine production rate are high. Numerical simulations are present to illustrate the theoretical predictions.

1. **Introduction.** According to the World Health Organization, cancer continues to be the second foremost cause of death globally, but how it develops and spreads is still not well understood. The most prevalent malignancies include prostate, breast, lung, colon, and rectum cancers. Approximately three percent of the deaths related to cancer are use of cigarettes, having a high body mass index, limited amounts of vegetables and fruits, drinking alcohol, and not physical activity. Numerous tumors can be treated if they are diagnosed early and treated appropriately [5]. When patients undergo tumor distortion, recurrence might still happen later. We must focus on both more effective treatment options and prevention measures.

A few treatments have been existing for a long time and are frequently utilized. They provide quick results by eliminating cancer cells, but there are significant downsides. In most situations, there is no selectivity for tumor cells, therefore they destroy healthy cells nearby. Further, the negative impacts are severe and might continue for a long time [7]. Different techniques are needed for treating different types of cancers. However, this is not the only situation since the diversity of a particular disease makes it impossible to follow a similar form of therapy even for individuals experiencing the same kind of cancer [8].

Immunotherapy is a rapidly increasing and expanding branch of cancer treatment. It focuses on improving patients' immune systems against cancer. Current immunotherapies include cytokines, inhibitors of checkpoints, targeted antigens, immunizations, adoptive cell transfer, and oncolytic bacteria, etc. To increase the

2020 *Mathematics Subject Classification.* Primary: 34C23, 34D20; Secondary: 92C37.

Key words and phrases. Tumor model, stability, center manifold, Hopf bifurcation, limit cycle.

This work was supported by the Natural Sciences and Engineering Research Council of Canada (No. R2686A02).

*Corresponding author: Pei Yu.

effectiveness of the therapy, they can be employed either alone or in conjunction with radiotherapies, chemotherapies, surgery, or targeted treatments. Immunotherapy involves using cytokines in combination with adoptive cellular immunotherapy (ACI) [8, 2]. A protein hormone known as cytokines plays an equally crucial role in native and adaptive immunity. Activated T cells primarily form cytokines during cell-mediated immune responses [6].

To distinguish the complex relations amongst the various aspects of the tumor microhabitat, mathematical modeling is a predominant tool. In this paper, we introduce a mathematical model describing the behaviors of the tumor cells, the $CD4^+$ T cells, and the cytokine interactions, in the form of ordinary differential equations (ODEs) [1], and focus on the study of the case with no treatment. We use a logistic growth function for the tumor cells, and Michaelis-Menten kinetics with various half-saturation values for all functional forms. Hopf bifurcation analysis is given to show the oscillating behaviours in the model. Numerical simulations are used to illustrate the theoretical predictions.

The remainder of the paper is organized as follows. In the next section, we will study the basic solution features of the proposed system. Then, we will discuss center manifold reduction in Section 3 and investigate the stability and bifurcations from equilibrium solutions in Section 4. Analysis on the codimension of Hopf bifurcation will be given in Section 4 to show the existence of maximal number of bifurcating limit cycles. Numerical simulations will be presented in Section 5, and finally conclusions will be drawn in Section 6.

2. **Modeling and reduction.**

In this section, we introduce a mathematical model describing the dynamical behaviors of the tumor cells, the $CD4^+$ T cells, and the cytokine interactions, and focus on the study for the case with no treatment. Let the densities of the tumor cells, $CD4^+$ T cells, and cytokine be denoted by x, y, and z, respectively. Then, the proposed model is described by the following ordinary differential equations (ODEs) [1]:

$$\begin{aligned} \frac{dx}{dt} &= xf(x) - d(x,z), \\ \frac{dy}{dt} &= g_y(x,y) - a_y(y) + I_1(t), \\ \frac{dz}{dt} &= g_z(x,y,z) - a_z(z) + I_2(t), \end{aligned} \tag{1}$$

where the function $f(x)$ represents the tumor cells per capita growth rate, $d(x,z)$ denotes the tumor cells loss caused by cytokines, $g_y(x,y)$ is the $CD4^+$ T cells proliferation through contacts with the tumor cells, and $g_z(x,y,z)$ denotes cytokines secretion by $CD4^+$ T cells. Apoptosis (natural death) of the $CD4^+$ T cells and the cytokine loss are denoted by the functions $a_y(y)$ and $a_z(z)$, respectively, while immunotherapy treatments are represented by $I_1(t)$ and $I_2(t)$, which may be time-dependent.

In this paper, a logistic growth function is utilized for the tumor cells, and Michaelis-Menten kinetics with various half-saturation values are used for all functional forms. As a result, it is anticipated that the tumor's development is reduced, as well as the tumor cells' ability to produce the $CD4^+$ T cells and an anticancer

cytokine. With these assumptions, model (1) can be rewritten as

$$\begin{aligned}\frac{dx}{dt} &= rx\Big(1-\frac{x}{K}\Big)-\frac{\delta xz}{m+x},\\ \frac{dy}{dt} &= \frac{\beta xy}{k+x}-ay+I_1,\\ \frac{dz}{dt} &= \frac{\alpha xy}{b+x}-\mu z+I_2,\end{aligned} \tag{2}$$

where all the parameters $r,\ K,\ m,\ a,\ b,\ k,\ \mu,\ \beta,\ \delta$, and α are positive constants, and $I_1(t)\geq 0$ and $I_2(t)\geq 0$ denote the regular remedies of the $CD4^+$ T cells and the cytokine in keeping with unit time, respectively. The parameters and their organic interpretations are summarized in Table 1.

TABLE 1. Parameters used in system (2) [1].

Parameter	Biological meaning	Unit
m	half saturation constant of the tumor-killing rate	cm^3
β	maximum $CD4^+$ T production rate	day^{-1}
k	half saturation constant of the $CD4^+$ T production rate	cm^3
a	death rate of the $CD4^+$ T cells	day^{-1}
b	half saturation constant of the cytokine production rate	cm^3
μ	cytokine loss rate	day^{-1}
r	growth rate of the tumor	day^{-1}
K	carrying capacity of the tumor	cm^3
δ	maximum tumor killing rate by cytokine	day^{-1}
α	maximum production rate of cytokine	day^{-1}
I_1	treatment by $CD4^+$ T	cm^3day^{-1}
I_2	treatment by cytokine	cm^3day^{-1}

In order to simplify the analysis in the following sections, we introduce the scaling

$$x=KX,\quad y=\frac{Kr^2}{\alpha\delta}Y,\quad z=\frac{Kr}{\delta}Z,\quad t=\frac{1}{r}\tau$$

into system (2) to obtain the dimensionless model

$$\begin{aligned}\frac{dX}{d\tau} &= X\Big(1-X-\frac{Z}{A+X}\Big),\\ \frac{dY}{d\tau} &= Y\Big(\frac{BX}{C+X}-D\Big)+I_1,\\ \frac{dZ}{d\tau} &= \frac{XY}{E+X}-FZ+I_2,\end{aligned} \tag{3}$$

where the six new positive parameters are defined as

$$A=\frac{m}{K},\quad B=\frac{\beta}{r},\quad C=\frac{k}{K},\quad D=\frac{a}{r},\quad E=\frac{b}{K},\quad F=\frac{\mu}{r}. \tag{4}$$

In this paper, we shall explore the dynamical behaviors of model (3) in the full 6-dimensional parameters space, particularly for the case without treatment, i.e., $I_1 = I_2 = 0$. Thus, system (3) is reduced to

$$\begin{aligned} \frac{dX}{d\tau} &= X\Big(1 - X - \frac{Z}{A+X}\Big), \\ \frac{dY}{d\tau} &= Y\Big(\frac{BX}{C+X} - D\Big), \\ \frac{dZ}{d\tau} &= \frac{XY}{E+X} - FZ, \end{aligned} \tag{5}$$

with the non-negative initial conditions:

$$X(0) = X_0 \geq 0, \quad Y(0) = Y_0 \geq 0, \quad Z(0) = Z_0 \geq 0. \tag{6}$$

We shall give an analysis on the generic dynamics of system (5) in terms of the 6-dimensional (A, B, C, D, E, F) parameter space. We pay particular attention on the analysis of Hopf and generalized Hopf bifurcation. We apply Hopf bifurcation theory to prove the existence of multiple limit cycles, giving rise to different types of bistable states. The new parameters and their biological meaning are given in Table 2.

TABLE 2. Parameters used in system (5).

Parameter	Biological meaning	value
A	half saturation constant of the tumor-killing rate	0.1
B	maximum $CD4^+$ T production rate	6
C	half saturation constant of the $CD4^+$ T production rate	1
D	death rate of the $CD4^+$ T cells	3
E	half saturation constant of the cytokine production rate	0.1
F	cytokine loss rate	5000

The dimensionless model (5) will be studied in the next several sections. We shall consider the property of solutions, the equilibria and their stability, and pay particular attention to the dynamics of the tumor celss, the $CD4^+$ T cells, and the cytokine interactions.

3. Property of solutions of system (5).

First, we consider the property of solutions of the system (5), and have the following result.

Theorem 3.1. *The solution of system (5) is positive if the given initial condition is positive and it is bounded.*

Proof. We begin by considering the well-posedness of the solutions of system (5). The existence and uniqueness of the solution of (5), subject to initial conditions (6), follow from the elementary theory of ODEs. We consider the solution of this initial value problem, $(X(\tau), Y(\tau), Z(\tau)) \in \mathbb{R}^3_+$. Since the variables represent densities and concentrations of physical quantities, the system must remain non-negative for all $\tau > 0$. We first consider the tumor equation. Using the variation principal, we obtain from the first equation in (5) that

$$X(\tau) = X(0)\, e^{\int_0^\tau [1 - X(s) - \frac{Z(s)}{A+X(s)}]\, ds},$$

which clearly indicates that $X(\tau) \geq 0$, for $\tau > 0$ if $X(0) \geq 0$. Similarly, it follows from the second equation in (5) that

$$Y(\tau) = Y(0)\, e^{\int_0^\tau [\frac{BX(s)}{C+X(s)} - D]\, ds},$$

implying that $Y(\tau) \geq 0$ for $\tau > 0$ if $Y(0) \geq 0$. Finally, the third equation in (5) gives

$$Z(\tau) = e^{-F\tau}\left[Z(0) + \int_0^\tau \left(\frac{X(s)Y(s)}{E + X(s)}\right) e^{Fs}\, ds\right].$$

This shows that $Z(\tau) > 0$ for $\tau > 0$ if $Z(0) \geq 0$, by noticing that $X(\tau) > 0$ and $Y(\tau) > 0$ for $\tau > 0$.

Next, we prove that the solution of system (5) is bounded. First of all, it is easy to see from the first equation in (5) that the following inequality holds:

$$\frac{dX}{d\tau} = X\Big(1 - X - \frac{Z}{A + X}\Big) \leq X(1 - X).$$

It is obvious that the solution of the DE: $\frac{dX}{d\tau} = X(1 - X)$ is bounded, and actually it converges to the equilibrium $X = 1$. Then, by the comparison principle, we know that X is bounded. Next, consider the variable Z. Suppose it is unbounded, i.e., $Z(\tau) \to +\infty$ as $\tau \to \infty$. Then, it follows from the first equation in (5) that $X(\tau) \to 0$ as $\tau \to \infty$, and thus the second equation in (5) yields $Y(\tau) \to 0$ as $\tau \to \infty$. Hence, the limit equation of the third equation in (5) becomes $\frac{dZ}{d\tau} = -\,F\,Z$, implying that $Z(\tau) \to 0$ as $\tau \to \infty$, leading to a contradiction. Therefore, Z is bounded. Finally, suppose Y is unbounded, i.e., $Y(\tau) \to +\infty$ as $\tau \to \infty$. Then, it follows from the third equation in (5) that $\frac{X(\tau)Y(\tau)}{E+X(\tau)} - FZ(\tau) \to +\infty$ as $\tau \to \infty$ since X and Z are bounded, yielding that $\frac{dZ(\tau)}{d\tau} \to +\infty$ as $\tau \to \infty$, giving $Z(\tau) \to +\infty$ as $\tau \to \infty$, a contradiction. Thus, Y is also bounded. □

4. **Equilibrium solutions and their stability.** Simply letting $\frac{dX}{d\tau} = \frac{dY}{d\tau} = \frac{dZ}{d\tau} = 0$ yields three equilibrium solutions:

Two boundary equilibria: $E_0 = (0, 0, 0),\ E_1 = (1, 0, 0)$;

One positive (interior) equilibrium:

$$E_2 = (X_2, Y_2, Z_2) = \left(\frac{CD}{B - D},\ \frac{F(E + X_2)Z_2}{X_2},\ (1 - X_2)(A + X_2)\right).$$

Define

$$B_t = (C + 1)D. \tag{7}$$

Then, we have the following theorem for the existence and stability of the equilibria.

Theorem 4.1. *For system (5), the two boundary equilibria E_0 and E_1 exist for all parameter values, while the positive equilibrium E_2 exists for $B > B_t$. E_0 is always a saddle-focus; E_1 is locally asymptotically stable (LAS) for $B < B_t$ and unstable for $B > B_t$, while E_2 is LAS for $B_t < B < B_H$ and unstable for $B > B_H$. A transcritical bifurcation happens between E_1 and E_2 at $B = B_t$, and a Hopf bifurcation occurs from E_2 at the critical point $B = B_H$, where B_H is defined in the proof.*

Proof. Since the two boundary equilibrium solutions are not related to any parameters, they exist for all parameter values. The positive equilibrium E_2 requires $Z_2 > 0$, that is, $X_2 = \frac{CD}{B-D} < 1$, yielding $B > B_t$.

The stability of the three equilibrium solutions can be easily determined from the Jacobian matrix of (5), evaluated at the equilibria. The Jacobian matrix of (5) is given by

$$J(X,Y,Z) = \begin{bmatrix} 1-2X-\dfrac{AZ}{(A+X)^2} & 0 & -\dfrac{X}{A+X} \\ \dfrac{BCY}{(C+X)^2} & \dfrac{BX}{C+X}-D & 0 \\ \dfrac{EY}{(E+X)^2} & \dfrac{X}{E+X} & -F \end{bmatrix}. \tag{8}$$

Evaluating J at the boundary equilibria E_0 and E_1, we have

$$J(E_0) = \begin{bmatrix} 1 & 0 & 0 \\ 0 & -D & 0 \\ 0 & 0 & -F \end{bmatrix} \quad \text{and} \quad J(E_1) = \begin{bmatrix} -1 & 0 & -\dfrac{1}{A+1} \\ 0 & \dfrac{B}{C+1}-D & 0 \\ 0 & \dfrac{1}{E+1} & -F \end{bmatrix}.$$

It is easy to see from $J(E_0)$ that the population-free equilibrium E_0 is a saddle-focus with a stable manifold lying on the non-negative Y-Z plane. This indicates that the tumor may not be eliminated without any treatment even if it is very small. The equilibrium E_1 is LAS for $B < B_t$, and unstable for $B > B_t$. A transcritical bifurcation occurs between E_1 and E_2 at the critical point $B = B_t$ (which will be shown next), but E_2 only exists for $B > B_t$.

Next, consider the stability of E_2. Note that the tumor size in E_2 is always smaller than the normalized carrying capacity 1 (the non-normalized carrying capacity is K). Evaluating the Jacobian matrix of system (5) at the positive equilibrium E_2, we obtain

$$J(E_2) = \begin{bmatrix} \frac{D[(A-2C-1)D-B(A-1)]C}{[(A-C)D-AB](B-D)} & 0 & \frac{CD}{(A-C)D-AB} \\ \frac{[(A-C)D-AB][(C+1)D-B][(C-E)D+EB]F}{C^2BD} & 0 & 0 \\ \frac{E[(A-C)D-AB][(C+1)D-B]F}{D[(C-E)D+BE]C} & \frac{CD}{(C-E)D+BE} & -F \end{bmatrix}. \tag{9}$$

A direct computation yields the characteristic polynomial for E_2

$$P_{E_2}(\lambda) = \lambda^3 + a_1\lambda^2 + a_2\lambda + a_3, \tag{10}$$

where

$$\begin{aligned} a_1 &= F + 1 - \frac{(B-B_t)[(A+2)CD + (B-B_t)A]}{[CD+B-B_t][(A+1)CD + (B-B_t)A]} \\ a_2 &= F - \frac{(B-B_t)CDF[(A+E+2)CD + (B-B_t)(A+E)]}{(CD+B-B_t)[(A+1)CD + (B-B_tA][(E+1)CD + (B-B_t)E]}, \\ a_3 &= \frac{DF(B-B_t)}{(1+C)D+B-B_t} \end{aligned} \tag{11}$$

It is easy to see that $a_3 > 0$ due to the existence condition $B > B_t$ for E_2. At the critical point $B = B_t$, $a_1 = F + 1 > 0$, $a_2 = F > 0$, and $a_3 = 0$, at which $E_2 = E_1$, implying that a transcritical bifurcation occurs between E_1 and E_2.

To simplify the analysis on the stability of E_2, we let

$$B = B_t + h, \quad (h \geq 0). \tag{12}$$

Then, the transcritial bifurcation point $B = B_t$ becomes $h = 0$. We want to consider the bifurcation from E_2 as h is increasing. Thus, substituting (12) into (11) yields

$$a_1(h) = F + 1 - h\,Q_1(h), \quad a_2(h) = F - h\,Q_2(h), \quad a_3(h) = h\,Q_3(h),$$

in which Q_1, Q_2, and Q_3 are given by

$$\begin{aligned}
Q_1(h) &= \frac{[(A+2)CD + hA]}{(CD+h)[(A+1)CD + hA]},\\
Q_2(h) &= \frac{CDF[(A+E+2)CD + h(A+E)]}{(CD+h)[(A+1)CD + hA][(E+1)CD + hE]},\\
Q_3(h) &= \frac{DF}{(1+C)D + h},
\end{aligned}$$

which clearly indicates that $Q_k(h) > 0$, $k = 1, 2, 3$ for $h > 0$. By the Routh-Hurwitz criteria, it is known that E_2 is LAS for $a_1(h) > 0$, $a_3(h) > 0$, and $\Delta_2(h) = a_1(h)a_2(h) - a_3(h) > 0$. At the critical point $h = 0$, $a_1 > 0$, $a_2 > 0$, $a_3 = 0$, and so $\Delta_2 > 0$. When h is increasing from $h = 0$, both a_1 and a_2 are decreasing from positive values, while a_3 is increasing from 0. Hence, $\Delta_2 = a_1a_2 - a_3$ crosses zero before either a_1 or a_2 does, implying that the only bifurcation which can happen from E_2 is Hopf bifurcation. Clearly, Bogdanov-Takes (B-T) bifurcation is not possible since it requires that $a_2 = a_3 = 0$. Further, to investigate if it is possible to have Hopf bifurcation from E_2, we derive the detailed expression for Δ_2 as follows:

$$\Delta_2(h) = F(F+1) - \frac{hFQ_4(h)}{(CD+h)^2[(A+1)CD+hA]^2[(C+1)D+h][(E+1)CD+hE]},$$

where

$$\begin{aligned}
Q_4(h) = {} & A^2E(D+1)h^5\\
& + AD\big[AC(5E+1)(D+1) + 2CE(D+1) + (A+C)E + (A+E)CF\big]h^4\\
& + CD^2(10A^2CDE + 4A^2CD + 10A^2CE + 4A^2CF + 8ACDE\\
& + 4ACEF + 5A^2C + 4A^2E + A^2F + 2ACD + 13ACE + AEF\\
& + 3ACF + CDE + CEF + A^2 + 2AC + 3AE + CE)h^3\\
& + C^2D^3(10A^2CDE + 6A^2CD + 10A^2CE + 6A^2CF + 12ACDE\\
& + 6ACEF + 9A^2C + 6A^2E + 3A^2F + 6ACD + 21ACE + 9ACF\\
& + 3AEF + 3CDE + 3CEF + 4A^2 + 10AC + 10AE + 3AF + CD\\
& + 5CE + 2CF + EF + 2A + E)h^2\\
& + C^3D^4(5A^2CDE + 4A^2CD + 5A^2CE + 4A^2CF + 8ACDE + 4ACEF\\
& + 7A^2C + 4A^2E + 3A^2F + 6ACD + 15ACE + 9ACF + 3AEF + 3CDE\\
& + 3CEF + 5A^2 + 14AC + 11AE + 6AF + 2CD + 7CE + 4CF + 2EF\\
& + 8A + 4C + 4E + 2F)h\\
& + C^4D^5(A+1)(ACDE + ACD + ACE + ACF + CEF + CDE + 2AC\\
& + AE + AF + CD + 3CE + 2CF + EF + 2A + 4C + 3E + 2F + 4).
\end{aligned}$$

It can be seen that $Q_4(0) = F(F+1) > 0$ and $\Delta_2 \to -\infty$ as $h \to \infty$ (since the coefficient of h^5 is positive), implying that $\Delta_2(h)$ has at least one positive root, and it may have multiple positive roots. The smallest root of $\Delta_2(h)$, denoted by h_H, defines a critical Hopf bifurcation point. In terms of the bifurcation parameter B, the Hopf critical point is given by $B_H = B_t + h_H$. Thus, the equilibrium E_2 is LAS for $B_t < B < B_H$ (or $0 < h < h_H$) and unstable for $B > B_H$. Hopf bifurcation occurs from E_2 at the critical point $B = B_H$.

This completes the proof for Theorem 4.1. □

Define the basic Reproduction number as

$$R_0 = \frac{B}{(C+1)D}. \tag{13}$$

Then, the dynamics and bifurcations of system (5) can be simply described as follows: The equilibrium E_0 is always a saddle-focus, the equilibrium E_1 is LAS for $R_0 < 1$ and unstable for $R_0 > 1$, while the equilibrium E_2 exists for $R_0 > 1$ and is LAS for $1 < R_0 < \frac{B_H}{(C+1)D}$, and unstable for $R_0 > \frac{B}{(C+1)D}$. A transcritical bifurcation happens between E_1 and E_2 at the critical point $R_0 = 1$, and Hopf bifurcation occurs from E_2 at the critical point $R_0 = \frac{B_H}{(C+1)D}$. Note that E_0 is a population-free equilibrium, E_1 is a disease-free equilibrium, and E_2 is an endemic equilibrium.

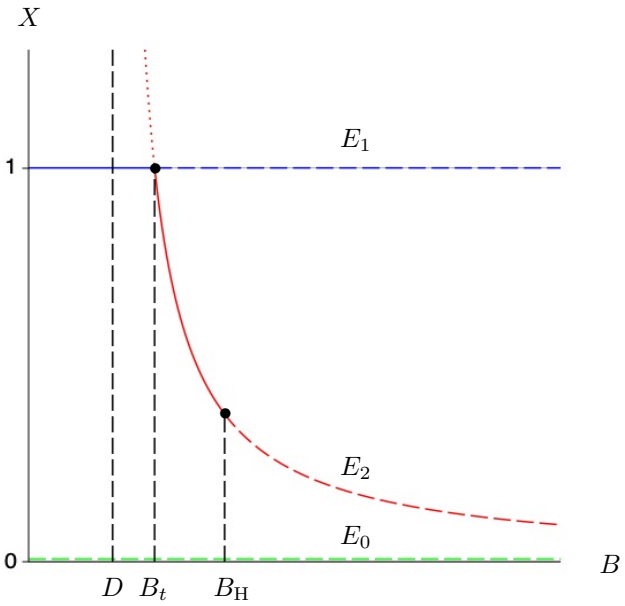

FIGURE 1. Bifurcation diagram for system (5) showing the equilibrium solutions E_0, E_1, and E_2, where solid and dashed lines/curves represent stable and unstable equilibrium solutions, respectively. The dotted curve of E_2 represents the solution that exists mathematically but is biologically meaningless, yielding negative Y.

The bifurcation diagram projected on the B-X plane for system (5) is shown in Figure 1, in which three equilibria E_0, E_1, and E_2 with stability are depicted. The transcritical bifurcation point B_t and the Hopf bifurcation point $B = B_H$ are specified.

To further explore the dynamics and bifurcation of system (5), we discuss two cases in the following: (1) $R_0 = 1$, for which we use center manifold theory to investigate the stability of equilibria, and (2) $R_0 > 1$, for which we consider Hopf bifurcation and pay particular attention to the codimension of the Hopf bifurcation.

4.1. **Case $R_0 = 1$ (or $D = \frac{B}{C+1}$).** When $R_0 = 1$ or $D = \frac{B}{C+1}$, system (5) is in a critical situation, i.e., the equilibria E_1 and E_2 coincide at the critical point $B = B_t$ and complex dynamics of the system happens on the center manifold, while the equilibrium E_0 is still a saddle-focus.

For this critical case, in order to keep the parameter B in the analysis, we treat D as a bifurcation parameter and change the equation $B = (C+1)D$ to $D = \frac{B}{C+1}$. Then, define $D_t = \frac{B}{C+1}$, at which $R_0 = 1$. At the critical point, the equilibrium solutions become

$$E_0 = (0, 0, 0), \quad E_1 = E_2 = (1, 0, 0). \tag{14}$$

We have following theorem.

Theorem 4.2. *For system (5) at the critical point $R_0 = 1$, the equilibria E_1 and E_2 coincide to become a degenerate stable node. There is no backward bifurcation for this critical case.*

Proof. Since at $R_0 = 1$ system (5) has a simple zero eigenvalue at E_1 $(= E_2)$, this implies that it is a degenerate node. To study the stability of E_1, we need to find the differential equation describing the dynamics on the center manifold, and then discuss the stability of E_1. To achieve this, we first perform a reduction analysis on the center manifold by introducing an affine transformation, given by

$$\begin{pmatrix} X \\ Y \\ Z \end{pmatrix} = \begin{pmatrix} 1 \\ 0 \\ 0 \end{pmatrix} + \begin{bmatrix} \frac{-1}{(E+1)(A+1)} & 1 & \frac{1}{A+1} \\ F & 0 & 0 \\ \frac{1}{E+1} & 0 & F-1 \end{bmatrix} \begin{pmatrix} u \\ v \\ w \end{pmatrix}, \tag{15}$$

into (5) with $D = \frac{B}{1+C}$ to obtain the system

$$\begin{aligned}
\frac{du}{d\tau} &= -\frac{CBu\big\{u - (E+1)\big[(A+1)v + w\big]\big\}}{(C+1)^2(A+1)(E+1)}, \\
\frac{dv}{d\tau} &= -v - v^2 - \frac{(AF+1)w^2}{(A+1)^3} - \frac{(AF+A+2)vw}{(A+1)^2} - \frac{u(P_1u - P_2v - P_3w)}{(A+1)^3(E+1)^3(C+1)^3(F-1)}, \\
\frac{dw}{d\tau} &= -Fw + \frac{u\big[CB(E+1) - (C+1)^2EF\big]\big\{u - (E+1)\big((A+1)v + w\big)\big\}}{(E+1)^3(A+1)(C+1)^2(F-1)},
\end{aligned} \tag{16}$$

where

$$\begin{aligned}
P_1 &= F\big(CB(A+1)(E+1)+(C+1)^2(1-AE)\big)-(E+1)(C+1)^2,\\
P_2 &= (E+1)(A+1)\big\{F\big[CB(A+1)(E+1)+(C+1)^2(A+E+2)\big]\\
&\quad -(A+2)(C+1)^2(E+1)\big\},\\
P_3 &= (E+1)\big\{(E+1)(C+1)^2(AF^2-2)\\
&\quad +\big[CB(A+1)(E+1)-(C+1)^2\big(A(1+2E)-E-2\big)\big]F\big\}.
\end{aligned}$$

Note that the linear part of system (16) is in Jordan canonical form, having eigenvalues 0, -1, and $-F$.

Then, applying center manifold theory and letting

$$v = a\,u^2, \quad w = b\,u^2,$$

and balancing the coefficients in the equations

$$\frac{dv}{d\tau} = 2\,a\,u\,\dot{u}, \quad \text{and} \quad \frac{dw}{d\tau} = 2\,b\,u\,\dot{u},$$

together with (16) yields

$$\begin{aligned}
a &= -\frac{(AEF+E-F+1)(C^2+1)+\big\{\big[\big((2-B)A-B\big)E-B(A+1)-2\big]F(E+1)\big\}C}{(A+1)^2(E+1)^3(C+1)^2(-1+F)},\\
b &= \frac{-C^2EF+CBE-2CEF+CB-EF}{(E+1)^2(A+1)(C+1)^2(-1+F)}.
\end{aligned}$$

Hence, the center manifold up to the second order is defined as

$$W^c = \{(u,v,w)|v = au^2+O(u^3), w = bu^2+O(u^3)\},$$

and the differential equation describing the dynamics on the center manifold is given by

$$\frac{du}{d\tau} = -\frac{CB}{(E+1)(C+1)^2(A+1)}\big\{u^2-\big[a(A+1)+b\big](E+1)u^3+O(u^4)\big\}, \quad (17)$$

which clearly indicates that the equilibrium E_1 is a stable degenerate node since the coefficient of u^2 is negative.

When $D = \frac{B}{1+C}$, the system still has four parameters, A, B, C, and D. We give a brief summary on the dynamics and bifurcation of system (5) at $R_0 = 1$. It can be seen from (17) that $u = 0$ defines a degenerate stable node on the center manifold. Now, system (5) has only two equilibria E_0 and E_1, and $Y_1 = 0$ still holds for the critical case. Back to the original equilibrium solution using (15), we have

$$X_1 = 1-\frac{u}{(1+E)(1+A)}, \quad (18)$$

which shows that $X_1 = 1$ when $u = 0$. The above stability for u implies that E_1 is a degenerate stable node, and so that no backward bifurcation can occur. Simulation of system (5) for the critical case $R_0 = 1$ is shown in Figure 2, indicating that all trajectories with different initial conditions converge to the degenerate node E_1. □

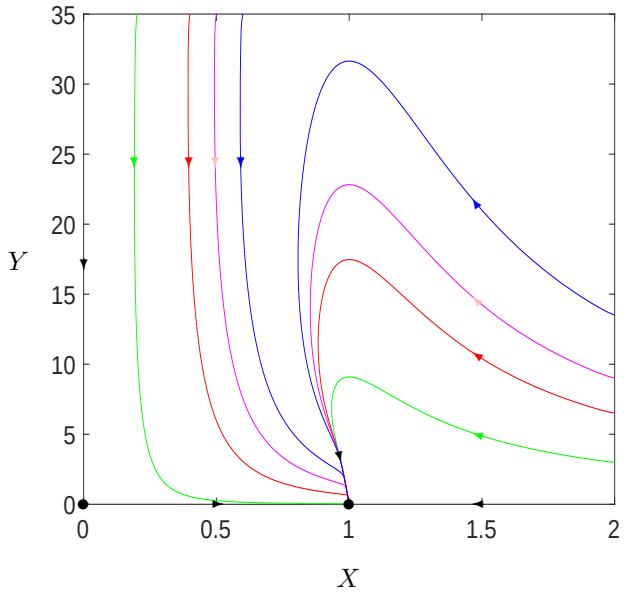

FIGURE 2. Phase portrait of system (5) at $R_0 = 1$, projected on the X-Y plane, showing the convergence of trajectories to the degenerate node $X = 1$ with the parameter values $A = \frac{1}{10}$, $B = \frac{29}{3}$, $C = 1$, $D = \frac{B}{1+C} = \frac{29}{6}$, $E = \frac{3}{1000}$, and $F = 100$.

4.2. **Case $R_0 > 1$ and codimension of Hopf bifurcation.** In this subsection, we consider the case $R_0 > 1$, and particularly investigate the codimension of the Hopf bifurcation discussed in the previous sections.

First, we describe the underlying concept of the technique used to study the codimension of Hopf bifurcation. The basic idea is to identify the dominate values that can be used to quantify the number of limit cycles bifurcating from a Hopf critical point and their stability for a given nonlinear dynamical system associated with a Hopf bifurcation. These dominant values are often known as focus values, and they may be derived by computing the normal forms for a general n-dimensional nonlinear systems. To be more specific, consider the following general n-dimensional autonomous differential system,

$$\dot{Z} = AZ + f(Z), \quad Z \in R^n, \quad f : R^n \to R^n, \tag{19}$$

where the linear and nonlinear components of the system are denoted by AZ and $f(Z)$, respectively. For our purpose, without loss of generality, assume that $f(0) = Df(0) = 0$, which indicates that the system's fixed point is $Z = 0$. In general, the matrix A may have eigenvalues with real parts that are negative, positive, or zero, and as a result, the system may contain stable, unstable, or center manifolds. To compute the normal form, the first step is typically to apply a linear transformation T to the given system, converting its linear portion to the Jordan canonical form, which is the system's normal form for the linear part. Thus, applying the linear transformation $Z = TX$ to the system results in the system,

$$\dot{X} = JX + f(X), \quad X \in R^n, \quad f : R^N \to R^N, \tag{20}$$

where $J = \text{diag}(J_1,\ J_2,\ J_3)$, in which J_1, J_2, and J_3 are in Jordan canonical forms, having zero, negative, and positive real parts, respectively. It should be noted that in real applications, the unstable manifold is usually assumed null since the system is unstable when it contains unstable manifold.

Now, based on system (20), we suppose that J_1 is two-dimensional and contains a pair of purely imaginary eigenvalues $\pm i\,\omega_c$ at a critical point, and J_3 is null. Then, we compute the normal form associated with Hopf and generalized Hopf bifurcations by employing center manifold theory, normal form theory, and computer algebra systems to to obtain the following normal form in polar coordinates [10]:

$$\begin{aligned} \frac{dr}{d\tau} &= r(v_0\mu + v_1 r^2 + v_2 r^4 + \cdots + v_k r^{2k} + \cdots), \\ \frac{d\theta}{d\tau} &= \omega_c + t_0 + t_1 r^2 + t_2 r^4 + \cdots + t_k r^{2k} + \cdots, \end{aligned} \tag{21}$$

where the motion's amplitude and phase are denoted by r and θ, respectively. The kth-order focus value is v_k $(k = 0, 1, 2, \dots)$. We can derive v_0 and t_0 using a linear analysis. The second equation in (21) can be used to calculate the frequency of the bifurcating periodic motion, whereas the first equation in (21) can be applied to examine bifurcation and the stability of limit cycles. When all the focus values are given in terms of the original system parameters, if we can use k parameters such that $v_0 = v_1 = \cdots = v_{k-1} = 0$ but $v_k \neq 0$ at the critical point specified by $\mu_c = (\mu_{1c}, ..., \mu_{kc})$, and the following condition holds:

$$\text{rank}\left[\frac{\partial(v_0, v_1, \cdots, v_{k-1})}{\partial(\mu_1, \mu_2, ..., \mu_k)}(\mu_c)\right] = k, \tag{22}$$

then the system can bifurcate k limit cycles around the origin (the equilibrium) from the Hopf critical point, by using appropriate perturbations on μ. More details on the topic of bifurcation of limit cycles can be found in [10, 4, 3].

We have the result for the codimension of Hopf bifurcation in the following theorem.

Theorem 4.3. *For system (5), when $C = 1$, $B = \frac{D(3-A)}{1-A}$ $(A < 1)$, the codimension of the Hopf bifurcation from the equilibrium E_2 is 4, implying that at least 4 small-amplitude limit cycles exist around the equilibrium E_2.*

Proof. Since the computation of the focus values is extremely complicated for the general case, we make a simplification by setting $C = 1$, $B = \frac{D(3-A)}{1-A}$ (with $A < 1$) in system (5), yielding the new system

$$\begin{aligned} \frac{dX}{d\tau} &= X\Big(1 - X - \frac{Z}{A+X}\Big), \\ \frac{dY}{d\tau} &= \frac{DY(2X - 1 + A)}{(1-A)(1+X)}, \\ \frac{dZ}{d\tau} &= \frac{XY}{E+X} - FZ, \end{aligned} \tag{23}$$

which has three equilibria:

$$\begin{aligned} E_0 &= (0, 0, 0), \\ E_1 &= (1, 0, 0), \end{aligned}$$

$$E_2 = \left(\frac{1-A}{2}, \frac{F(A+1)^2(1-A+2E)}{4(1-A)}, \frac{(A+1)^2}{4}\right).$$

Since we are interested in the Hopf bifurcation which occurs from E_2, we similarly use the Jacobian matrix of the system to determine the stability of E_2, which produces

$$J(E_2) = \begin{bmatrix} 0 & 0 & \frac{A-1}{A+1} \\ \frac{DF(A+1)^2(A-2E-1)}{(A-3)(A-1)^2} & 0 & 0 \\ \frac{E(A+1)^2F}{(A-1)(A-2E-1)} & \frac{A-1}{A-2E-1} & -F \end{bmatrix},$$

yielding the characteristic polynomial

$$P_{E_2}(\lambda)) = \lambda^3 + a_1\lambda^2 + a_2\lambda + a_3,$$

where

$$a_1 = F, \quad a_2 = \frac{F(A+1)E}{1-A+2E}, \quad a_3 = \frac{FD(A+1)}{3-A},$$

showing that all a_i's are positive. To find a Hopf bifurcation critical point, we choose E as the bifurcation parameter, and let

$$\Delta_2 = F(A+1)\,\frac{E\big[F(3-A)-2D\big] - D(1-A)}{((3-A)(1-A+2E)} = 0,$$

from which we find the Hopf critical point defined as

$$E_H = \frac{D(1-A)}{F(3-A)-2D}.$$

Since $A < 1$ and $E \gg D$, we know that $E_H > 0$. Thus, the equilibrium E_2 is LAS for $E > E_H$, and unstable for $0 < E < E_H$. Hopf bifurcation occurs from E_2 at the critical point $E = E_H$.

To compute the focus values for system (23) at $E = E_H$, we introduce the following affine transformation,

$$\begin{pmatrix} X \\ Y \\ Z \end{pmatrix} = \begin{pmatrix} \frac{1-A}{2} \\ \frac{F(A+1)^2(A-1-2E)}{4(A-1)} \\ \frac{(A+1)^2}{4} \end{pmatrix} + \begin{bmatrix} 0 & \frac{(1-A)\sqrt{D_2(3+2A-A^2)}}{(1+A)^2D_2} & \frac{1-A}{F(A+1)} \\ \frac{F^2(3-A)}{F(3-A)-2D_2} & 0 & \frac{-D_2(1+A)}{F(3-A)-2D_2} \\ 1 & 0 & 1 \end{bmatrix} \begin{pmatrix} u \\ v \\ w \end{pmatrix},$$

where $D_2 = \sqrt{D}$, into (23) to obtain the system whose linear part is in Jordan canonical form:

$$\begin{aligned}
\frac{du}{d\tau} &= \omega_c v + \frac{(2F^3-2DF)A^2+(-8F^3-4D^2+4DF)A+6F^3-4D^2+6DF}{(A+1)(A-3)F((D-F^2)A+3F+D)}u^2 \\
&\quad + \frac{2(-AF^2+AD+2DF+F^2+D)D}{F^2(-AF^2+AD+3F^2+D)(-3+A)}w^2+\cdots, \\
\frac{dv}{d\tau} &= -\omega_c u + V_{11}v^2 + V_{12}w^2+\cdots, \\
\frac{dw}{d\tau} &= -Fw + \frac{4(D-F)F}{F(-AF^2+AD+3F^2+D)(A+1)}v^2 \\
&\quad - \frac{4(D-F)D}{F(-AF^2+AD+3F^2+D)(A-3)}w^2+\cdots,
\end{aligned} \tag{24}$$

in which

$$\omega_c = \sqrt{\frac{D(A+1)}{3-A}},$$

while other lengthy expressions denoted by $\cdots$ are omitted for simplicity. $V_{11} = \frac{V_{11n}}{V_{11d}}$ and $V_{12} = \frac{V_{12n}}{V_{12d}}$ with

$$\begin{aligned}
V_{11n} =& (D-F^2)A^4 + 4(2F^2-D)A^3 + 2[11F^2-(2D^2+2F+1)D]A^2 \\
&+ 4[6F^2-2D^2+(2F+1)D]A - 4D^2 + (4F-3)D - 9F^2), \\
V_{11d} =& \omega_c(A+1)^2((-F^2+D)A+3F^2+D), \\
V_{12n} =& -D\big\{(D-F^2)A^4 - 4[F^3-2F^2-(F-1)D]A^3 \\
&+ 2[12F^3-11F^2-2D^2-(2F-1)D]A^2 \\
&- 4[9F^3-6F^2+2D^2+(F-1)D]A - 4D^2+(4F-3)D-9F^2\big\}, \\
V_{12d} =& \omega_c(A+1)(A-3)F^2[(D-F^2)A+3F^2+D].
\end{aligned}$$

Now, we apply the Maple program in [10] for computing the normal forms associated with Hopf and generalized Hopf bifurcations to get the amplitude equation in the normal form up to the 9th-order as follows:

$$\frac{dr}{d\tau} = r[v_0\mu + v_1 r^2 + v_2 r^4 + v_3 r^6 + v_4 r^8 + O(r^{10})], \tag{25}$$

where $\mu = E - E_H$ is a perturbation parameter, and v_0, v_1, v_2, v_3, and v_4 are the 0th-order, 1st-order, 2nd-order, 3rd-order, and 4th-order focus values.

The transversal condition is obtained by using a linear analysis as

$$v_0 = -\frac{(1+A)[(A-3)F+2D]^2}{2(1-A)(3-A)[(3-A)F^2+(1+A)D]} < 0, \tag{26}$$

indicating that E is decreasing to cross the Hopf critical point $E = E_H$, which agrees with the above result: E_2 is LAS for $E > E_H$, and unstable for $E < E_H$.

The equation (25) can be utilized to do bifurcation analysis, and the sign of v_1 indicates whether the Hopf bifurcation is supercritical or subcritical, while the signs of higher-order focus values can determine the stability of multiply bifurcating limit cycles. The general necessary and sufficient condition for the existence of multiple limit cycles is given in (22). For our system (24), using the Maple program [10], we

obtain the focus values v_1, v_2, v_3, and v_4 as follows:

$$
\begin{aligned}
v_1 &= \frac{(1-A)(3-A)v_{1a}}{16D(A+1)^4[(A-3)F+2D][(3-A)F^2+(A+1)D][(3-A)F^2+4(A+1)D]},\\
v_2 &= \frac{(A-1)v_{2a}}{144v_{2d}},\\
v_3 &= \cdots,\\
v_4 &= \cdots,
\end{aligned}
$$

where

$$
\begin{aligned}
v_{1a} =& (3A^2-6A-1)(A-1)^2(A-3)^3F^5+4D(3A-5)(A-3)(A+1)^2F^4\\
&-D(A+1)(A-3)\big[4(A+1)(A-7)D+(A-1)^2(A-3)(15A^2-26A-1)\big]F^3\\
&-4D^2(A+1)^2\big[2D(A+1)(A-3)-A^4+8A^3-20A^2+4A-31\big]F^2\\
&-4D^2(A+1)^2\big[8(A+4)(A+1)D+(3A-1)(3-A)(A-1)^3\big]F\\
&+8D^3(A+1)^3\big[5D(A+1)-(A-3)(A-1)^2\big],\\
v_{2a} =& \cdots,\\
v_{2d} =& D^3F^2(A+1)^{10}[(A-3)F+2D][D(9A+9)+F^2(3-A)]\\
&\times[D(A+1)+F^2(3-A)]^3[4D(A+1)+F^2(3-A)]^3
\end{aligned}
$$

The lengthy expressions for v_{2a}, v_3, and v_4 are omitted here for brevity.

Since the v_ks contain 3 parameters, A, D, and F, it might be possible to have solutions such that $v_1 = v_2 = v_3 = 0$, but $v_4 \neq 0$, yielding at most 4 limit cycles. Based on the focus values v_1, v_2, and v_3, we first use the Maple-built command *eliminate* to get a solution $D(A,F)$ and two resultants: $R_1(A,F) = R_0(A,F)\,R_{1a}(A,F)$ and $R_2(A,F) = R_0(A,F)R_{2a}(A,F)$, where

$$
\begin{aligned}
R_0(A,F) =& F(1-A)(3-A)[1+3A(2-A)][1+A+(3-A)F]\\
&\times[4(1+A)+(3-A)F]\big\{(3-A)\big[8F^2-(1-A)^2)\big]+(A+17)F\big\}\\
&\times\big\{(3-A)\big[F^2+4(1-A)^2\big]+4(1+5A)F\big\}>0, \quad (\text{for} \quad A<1<F).
\end{aligned}
$$

$R_{1a}(A,F)$ and $R_{2a}(A,F)$ are two lengthy polynomials in A and F. Then, we use the Maple-built command *resultant* to obtain a lengthy resultant polynomial in A:

$$
R_{12}(A) = -C_0(1-A)^5 62(3-A)^4 80(1+6A-3A^2)^1 0R_{12a}\,R_{12b}\,R_{12c}\,R_{12d}\,R_{12e},
$$

where C_0 is a big integer, and

$$
\begin{aligned}
R_{12a} =& (A^6-21A^5+100A^4-174A^3+117A^2-77A+22)\\
&\times(A^8-34A^7+262A^6-850A^5+1344A^4-758A^3+810A^2-22A+15)\\
&\times(692356A^8-8273296A^7+38723436A^6-86480443A^5+93238801A^4\\
&-34912614A^3-19718394A^2+10915137A+3619593),
\end{aligned}
$$

$$
\begin{aligned}
R_{12b} = {} & 21472041204A^{16} - 478685886756A^{15} + 4655191749410A^{14} \\
& -34305698817233A^{13} + 215384167112585A^{12} - 969873671993323A^{11} \\
& +2873132220801823A^{10} - 5219368638878410A^{9} + 4808258364989540A^{8} \\
& -6318448391071 46A^{7} - 1746598670362432A^{6} + 369616640399739A^{5} \\
& +316560031040433A^{4} - 78293927207799A^{3} - 8702697485457A^{2} \\
& +2044756430064A + 188337117438, \\
R_{12c} = {} & 167799312A^{16} - 3958473216A^{15} + 42320529064A^{14} \\
& -271935782032A^{13} + 1172853133196A^{12} - 3585911951970A^{11} \\
& +7985864531153A^{10} - 13061138801753A^{9} + 15498297078232A^{8} \\
& -12684785748056A^{7} + 5940193043694A^{6} + 296535775826A^{5} \\
& -2874589615504A^{4} + 2350575838674A^{3} - 1033536360511A^{2} \\
& +259226146431A - 30413518092, \\
R_{12d} = {} & 90882A^{22} - 2679318A^{21} + 35478081A^{20} - 277959600A^{19} \\
& +1424448720A^{18} - 4950964386A^{17} + 11507199649A^{16} \\
& -15822195200A^{15} + 3505374380A^{14} + 38022655684A^{13} \\
& -98266484414A^{12} + 143736947488A^{11} - 150810106072A^{10} \\
& +126898351068A^{9} - 91109565046A^{8} + 54088899456A^{7} \\
& -23425253534A^{6} + 6141349874A^{5} - 727614883A^{4} \\
& +53692176A^{3} - 25228552A^{2} + 5826598A + 882677, \\
R_{12e} = {} & \cdots, \\
R_{12f} = {} & \cdots,
\end{aligned}
$$

where R_{12e} and R_{12f} are respectively 386-degree and 1908-degree polynomials in A. It is easy to verified that R_{12c} and R_{12d} have no real solutions for $A \in (0,1)$, while R_{12a}, R_{12b}, and R_{12e} have only 9 real solutions for $A \in (0,1)$. Then, we use these 9 solutions to obtain 4 positive solutions for F. Among these 4 sets of solutions (A_k, F_k), $k = 1,2,3,4$, we use the above obtained formula $D(A,F)$ to verify that only one solution satisfies $D > 0$. This unique solution is given by

$$
\begin{aligned}
& A = 0.9434673546\cdots, \quad B = 154.3184037325\cdots, \quad C = 1, \\
& D = 4.2421050801\cdots, \quad E = 0.4459655614\cdots, \quad F = 5.6930540630\cdots,
\end{aligned} \tag{27}
$$

where $E = E_H$. Note that 1000-digit point accuracy has been used in the above computations in order to guarantee the correctness of conclusion. With this solution, we have

$$
\omega_c = 0.2053782428\cdots, \quad v_0 = v_1 = v_2 = v_3 = 0, \quad v_4 = 0.1785278748\cdots \times 10^{-7} \neq 0,
$$

which shows that system (5) can have at most 4 small-amplitude limit cycles arising from Hopf bifurcation. Finally, we check the formula in (22) to obtain

$$
\operatorname{rank}\left[\frac{\partial(v_1, v_2, v_3)}{\partial(A, D, F)}\right]_{(27)} = -0.2636627563\cdots \times 10^{-14} < 0,
$$

which indeed shows that 4 small-amplitude limit cycles can bifurcate from E_2 near the critical point defined in (27). Note that v_0 is excluded in the above formula since $E = E_H$ has separately solved the equation $v_0 = 0$.

The proof of Theorem 4.3 is complete. □

5. **Numerical simulation.** In this section, we use numerical simulation to demonstrate the theoretical results obtained in the previous sections. However, it should be pointed out that realizing the bifurcation of 4 small-amplitude limit cycles using numerical simulation is extremely difficult. In fact, to the best of our knowledge, so far in the literature, the limit cycle simulation is only successful for 3 limit cycles, for example, see [11]. We shall present two simulations, one for one limit cycle, and the other for two limit cycles. The bifurcation diagrams for these limit cycle bifurcations are shown in Figure 3.

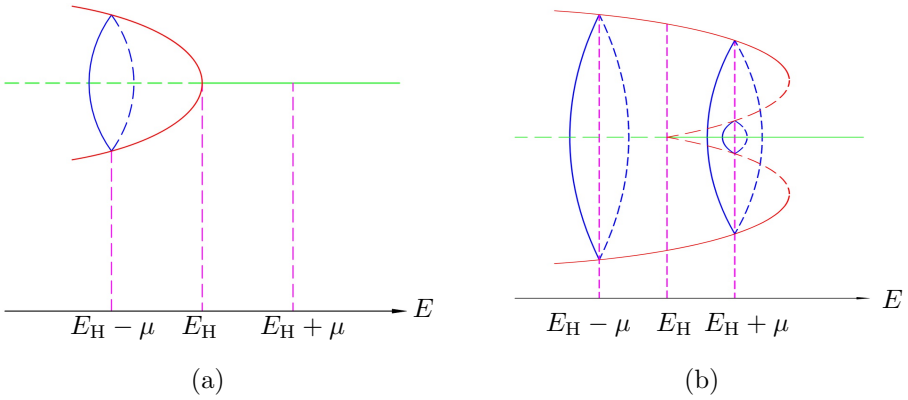

FIGURE 3. Bifurcation diagram for Hopf bifurcations of system (5) yielding (a) one limit cycle bifurcating at $E = E_H - \mu$; and (b) two limit cycles bifurcating at $E = E_H + \mu$.

We take the following parameter values for simulation of one stable limit cycle, as shown in Figure 4(a):

$$A = 0.1, \quad B = 9.666667, \quad C = 1, \quad D = 3, \quad E = 0.003, \quad F = 100.$$

To show the existence of two limit cycles, we choose $A = 0.9$ and $F = 20$, and then solve $v_1 = 0$ to get $\sqrt{D} = 3.69021284$. Further, taking the perturbation on $\sqrt{D}$ as $\sqrt{D} = 3.69021284 + 0.0001$, leading to $D = 13.6176708$ and $E_H = 0.09223153$, which yields one small-amplitude limit cycle. To get one more small limit cycle, we take $\mu = 0.2 \times 10^{-10}$ to get

$$v_0\mu = -0.22778579 \times 10^{-10}, \quad v_1 = 0.18776581 \times 10^{-7}, \quad v_2 = -0.32816726 \times 10^{-5},$$

which yields the following normal form equation for the amplitudes of bifurcating limit cycles:

$$\frac{dr}{d\tau} = r\big[v_0\,\mu + v_1 r^2 + v_2 r^4 + O(r^6)\big].$$

Solving the above equation, we obtain the approximate solutions for the amplitudes of the two limit cycles: $r_1 \approx 0.041783$ and $r_2 \approx 0.063054$.

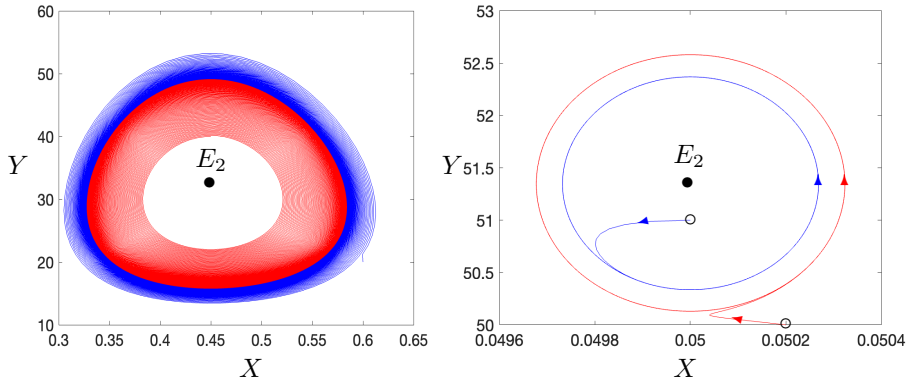

FIGURE 4. Simulated limit cycles for system (5): (a) one stable limit cycle for $A = 0.1$, $B = 9.666667$, $C = 1$, $D = 3$, $E = 0.003$, $F = 100$; and (b) two limit cycles for $A = 0.9$, $B = 285.971087$, $C = 1, D = 13.617671$, $E = 0.092232$, $F = 20$, with the outer one stable and the inner one unstable, both enclosing the stable equilibrium E_2.

The simulated limit cycles are shown in Figure 4. Figure 4(a) depicts one stable limit cycle. Two trajectories (in red and blue colors) start from two initial points, one is outside the limit cycle, and one is inside the limit cycle. Both converge to the limit cycle (the intersection of the red and blue trajectories), which encloses the unstable equilibrium E_2. Bifurcation of two limit cycles is given in Figure 4(b), where only the bigger limit cycle is shown since the existence of the small limit cycle is due to that both the bigger limit cycle and the equilibrium E_2 are stable (E_2 is stable because $v_0\mu < 0$). Again, two initial points (marked by the two circles in Figure 4(b)) are chosen from outside and inside the bigger stable limit cycle. However, due to extremely slow convergence, unlike Figure 4(a), it does not show the two trajectories converging to the exact bigger stable limit cycle, but it clearly indicates the direction of convergence.

6. **Conclusion.** In this paper, a mathematical model consisting of tumor cells, $CD4^+$ T cells, and cytokine relations has been studied for examining how the $CD4^+$ T cells might influence tumor reduction and latency. Although the $CD4^+$ T cells do not directly destroy the tumor cells, they can produce and deploy cytokines to modulate tumor growth. We apply stability and bifurcation theory to investigate the stability of equilibria and the oscillating behaviors arising from Hopf bifurcation. Center manifold theory and normal form theory are employed to study bifurcation of limit cycles. The bifurcation results obtained in this paper indeed indicate that the model can have complex dynamical behaviors, which may be more proper to describe the real situation.

Our study shows that the tumor cells persist when no treatment is applied, irrespective of the size of the tumor. In the current study, the $CD4^+$ T cells are treated as a single type and the simplest tumor-suppressing cytokine. No direct relations are assumed between the tumor and $CD4^+$ T cells. It is shown that,

without treatment, a patient with very low tumor antigenicity would experience tumors expanding to its maximum size, regardless of whether the tumor destruction rate and the cytokine production rate are high [9]. On the other hand, if either of the tumor-killing rate or the cytokine production rate is high, but the maximum $CD4^+$ T production rate is not excessively low, tumor recurrence can happen, and its size can be managed to a smaller extent. However, complete elimination of the tumor is not possible without intervention. In order to completely eliminate tumor cells while the $CD4^+$ T cells are administered, we aim to assess if immunotherapy itself is adequate in the future research.

REFERENCES

[1] L. Anderson, S. Jang and J. L. Yu, Qualitative behaviour of system of tumor-$CD4^+$-cytokine interactions with treatments, *Math. Meth. Appl. Sci.*, **38** (2015), 4330-4344.

[2] R. Eftimie, J. L. Bramson and D. J. D. Earn, Interactions between the immune system and cancer: A brief review of non-spatial mathematical models, *Bull. Math. Biol.*, **73** (2011), 2-32.

[3] M. Han and P. Yu, *Normal Forms, Melnikov Functions, and Bifurcations of limit cycles*, Springer-Verlag, New York, 2012.

[4] J. Jiang and P. Yu, Multistable phenomena involving equilibria andperiodic motions in predator-prey systems, *Int. J. Bifurcation and Chaos*, **27** (2017), 1750043, 28 pp.

[5] A. M. Knowles and J. P. Selby, *Introducation to the Cellcular and Molecular Biolody of Cancer, (4th ed.)*, Oxford University Press Inc. New York, 2005.

[6] G. E. Mahlbacher, K. C. Reihmer and H. B. Frieboes, Mathematical modeling of tumor-immune cell interactions, *J. Theor. Biol.*, **469** (2019), 47-60.

[7] B. Mansoori, A. Mohammadi, S. Davudian, S. Shirjang and B. Baradaran, The different mechanisms of cancer drug resistance: A brief review, *Adv. Pharm. Bull.*, **7** (2017), 339-348.

[8] P. Parsonidis and I. Papasotiriou, Adoptive cellular transfer immunotherapies for cancer, *Cancer Treat. Res. Commun.*, **32** (2022), 100575.

[9] H. C. Wei, J. L. Yu and C. Y. Hsu, Periodically pulsed immunotherapy in a mathematical model of Tumor, $CD4^+$ T cells, and antitumor cytokine interactions, *Comput. Math. Methods Med.*, (2017), 2906282, 12 pp.

[10] P. Yu, Computation of normal forms via a perturbation technique, *J. Sound Vib.*, **211** (1998), 19-38.

[11] W. Zhang, L. M. Wahl and P. Yu, Modelling and anlysis of recurrent autoimmune disease, *SIAM J. Appl. Math.*, **74** (2014), 1998-2025.

Received August 2024; revised April 2025; early access May 2025.